Electronic Excitations in Bi2Sr2CaCu208: Fermi Surface, Dispersion, and Absence of Bilayer Splitting

doi: 10.1103/PhysRevLett.76.1533

Electronic Excitations in $Bi_2Sr_2CaCu_2O_8$: Fermi Surface, Dispersion, and Absence of Bilayer Splitting

H. Ding,[1,2] A. F. Bellman,[1,3] J. C. Campuzano,[1,2] M. Randeria,[1] M. R. Norman,[1] T. Yokoya,[4] T. Takahashi,[4] H. Katayama-Yoshida,[4] T. Mochiku,[5] K. Kadowaki,[5] G. Jennings,[1] and G. P. Brivio[3]

[1]*Materials Sciences Division, Argonne National Laboratory, Argonne, Illinois 60439*

[2]*Department of Physics, University of Illinois at Chicago, Chicago, Illinois 60607*

[3]*Dipartimento di Fisica, Universita di Milano, 20133 Milano, Italy*

[4]*Department of Physics, Tohoku University, 980 Sendai, Japan*

[5]*National Research Institute for Metals, Sengen, Tsukuba, Ibaraki 305, Japan*

(Received 5 July 1995)

From a detailed study, including polarization dependence, of the normal state angle-resolved photoemission spectra for $Bi_2Sr_2CaCu_2O_8$, we find only one CuO_2 band related feature. All other spectral features can be ascribed either to umklapps from the superlattice or to "shadow bands." Even though the dispersion of the peaks looks like band theory, the line shape is anomalously broad and no evidence is found for bilayer splitting. We argue that the "dip feature" in the spectrum below T_c arises not from bilayer splitting, but rather from many-body effects.

PACS numbers: 74.72.Hs, 71.18.+y, 74.25.Jb, 79.60.Bm

It is now well established that, in spite of their many unusual properties above T_c, the cuprate superconductors (SC) exhibit a Fermi surface in their normal state as probed by angle-resolved photoemission spectroscopy (ARPES) [1–3]. In this paper we examine in detail ARPES data on $Bi_2Sr_2CaCu_2O_8$ (Bi2212) with an aim to clearly distinguish aspects of these data which can be discussed within a one-particle band theory framework from those which are dominated by many-body effects.

We will first show that the observed normal state spectral peaks can be classified as arising from three sources: (1) the main planar CuO_2 band, (2) umklapp bands related to the structural superlattice, and (3) "shadow bands" [4]. We discuss in detail polarization selection rules in the presence of the superlattice, which allows us to resolve previously puzzling and apparently conflicting features of the ARPES data above and below T_c.

One of the most remarkable features of the data is the absence of any observable bilayer splitting. On very general grounds, one expects that the two CuO_2 layers in a unit cell of Bi2212 should hybridize to produce a bonding and an antibonding band, but we find no evidence for these two bands. Since the normal state spectra are very broad, one might not be able to resolve the two bands. We show, however, that even for $T \ll T_c$, where the spectral function has a sharp, resolution-limited peak, there is no evidence for the bilayer splitting. We note that the absence of bilayer splitting was predicted early on by Anderson [5], who argued that this was a signature of nontrivial many-body effects.

Using the photon polarization dependence of the data we argue that the dip feature [3,6] is part of a single spectral function, and does not arise from two separate spectral peaks as might be expected for bilayer-spilt bands. We further argue that the dip has a natural explanation in terms of electron-electron interactions. Finally, we briefly contrast Bi2212 data with ARPES data on other bilayer materials: $YBa_2Cu_3O_7$ [7] and $YBa_2Cu_4O_8$ [8], which are thought to show two "bands."

The results presented below depend crucially on very high quality single crystals ($T_c = 87$ K) which were used in our earlier studies [9,10]. Details about the samples and the experimental procedure may be found in [9]. A representative set of normal state ($T = 95$ K) energy distribution curves (EDC's) obtained along various principal symmetry directions in Bi2212 are shown in Fig. 1. We use the notation $\Gamma = (0,0)$, $\overline{M} = (\pi,0)$, $X = (\pi,-\pi)$, and $Y = (\pi,\pi)$, where $\Gamma\overline{M}$ is along the CuO_2 bond direction. One can see several peaks dispersing with momentum and crossing the Fermi energy E_F (the zero of binding energy). Before discussing each panel of Fig. 1

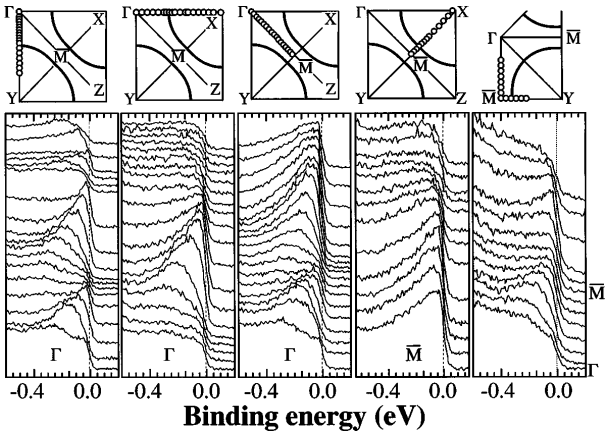

FIG. 1. Normal state ($T = 95$ K) EDC's of Bi2212 along various symmetry lines at values of the momenta shown as open circles in the upper insets. The photon polarization **A** is horizontal in each panel.

in detail we describe Fig. 2, which will help to give an overview of the main results derived from Fig. 1.

In Fig. 2(a) we show data points corresponding to various E_F crossings; the locus of these crossings defines the Fermi surface (FS). To determine FS location we use the rough criterion that the integrated area of the dispersing part of the spectrum, which is proportional to the momentum distribution $n(\mathbf{k})$ [10], falls to one-half its maximum value at $\mathbf{k}_F$. At a few selected points we have checked that we got very similar $\mathbf{k}_F$ results from a peak in $|\nabla_{\mathbf{k}} n(\mathbf{k})|$.

The dispersion of the spectral peak positions are plotted in Fig. 2(b). While it is convenient to use the language of band theory to describe these dispersing features, it must be noted that the normal state line shapes are very broad with a width (imaginary part of the self-energy) comparable to their peak energy. Also, the peak position incorporates shifts due to the real part of the self-energy and does not represent the "bare" band structure.

In addition to the peak position data points in Fig. 2(b), we also plot several curves. The thick curve is a six-parameter tight-binding fit [11] to the Y-quadrant data; this represents the main CuO_2 band. The two thin curves are obtained by shifting the main band fit by $\pm\mathbf{Q}$, respectively, where $\mathbf{Q} = (0.21\pi, 0.21\pi)$ is the superlattice (SL) vector known from structural studies [12]. These SL umklapp bands could arise either from the effect of the Bi-O SL distortion on the CuO_2 plane or, alternatively, from the exiting photoelectron diffracting off the Bi-O SL. Below we will present polarization evidence which favors the latter explanation. We also show a dashed curve which is a (π, π) foldback of the main band fit; this shadow band will be discussed below.

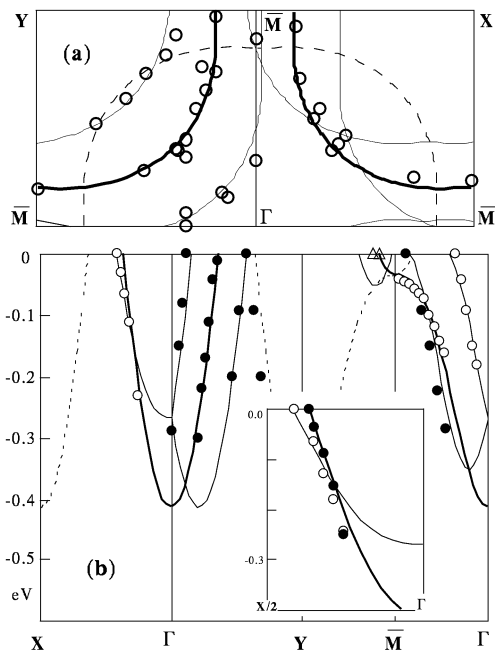

FIG. 2. (a) Fermi surface and (b) dispersion obtained from normal state measurements. The thick lines are obtained by a tight binding fit to the dispersion data of the main band with the thin lines $(0.21\pi, 0.21\pi)$ umklapps and the dashed lines (π, π) umklapps of the main band. Open circles in (a) are the data. In (b), filled circles are for odd initial states (relative to the corresponding mirror plane), open circles for even initial states, and triangles for data taken in a mixed polarization geometry. The inset of (b) is a blowup of ΓX.

The Fermi surfaces corresponding to the fits in Fig. 2(b) are shown as curves in Fig. 2(a): the main FS sheet is a thick line, the two umklapp sheets are thin lines, and the shadow band FS is dashed. The evidence for the SL bands and corresponding FS's is very direct in the Y quadrant. We will show below that a detailed study of spectra along ΓX gives convincing evidence for SL effects in the X quadrant. Finally, we note that the area enclosed by the main FS corresponds to a hole doping of 0.17, the same as that for optimally doped LaSrCuO.

We now return to the EDC's of Fig. 1 and discuss each panel in detail with special emphasis on the polarization selection rules. Note that the photon polarization $\mathbf{A}$ is horizontal for each panel. The first panel [Fig. 1(1)] shows EDC's along ΓY at an incident photon energy $h\nu = 19$ eV. The main band and the $\pm\mathbf{Q}$ umklapp features are clearly visible in the data. Some data points fall on the dashed curve in Fig. 2(b) giving evidence for the shadow band below E_F. For $h\nu = 22$ eV (data not shown) we find that the main band signal is enhanced, the umklapp intensities are diminished, and the shadow bands cannot be observed, presumably due to matrix element effects. Their sensitive photon energy dependence, together with the absence of a strong feature very close to E_F, might explain why the shadow bands were not seen in the EDC mode experiments prior to Aebi *et al.* [4]. These shadow bands may be either of magnetic origin [13] or of structural origin [14].

The polarization in Fig. 1(1), denoted by $\Gamma Y\perp$, is such that only initial states odd with respect to a reflection in the ΓY mirror plane lead to dipole-allowed transitions. In contrast, no dispersing features are seen in the $\Gamma Y\|$ geometry (data not shown). Thus the Y-quadrant data are consistent with emission from a one-particle orbital with $d_{x^2-y^2}$ symmetry about a Cu site. However, the X-quadrant data do not show these selection rules. This apparent violation of selection rules along ΓX, which was observed before [3,15], can now be understood in terms of the SL umklapp bands.

We see a clearly dispersing spectral peak in the $\Gamma X\|$ geometry ($h\nu = 22$ eV) in the second panel [Fig. 1(2)]. The initial state must be even about ΓX, and thus cannot be the main CuO_2 band (thus the "hump" observed in the superconducting gap near ΓX is a superlattice effect [16]). However, there is an even linear combination of the two SL bands which can contribute; it is given by $\psi(\mathbf{k} + \mathbf{Q}) - \psi(\mathbf{k} - \mathbf{Q})$, where $\mathbf{k}$ is the wave vector along ΓX and $\mathbf{Q}$ the SL vector. To further check this we have carefully measured the dispersions in the $\Gamma X\|$ and the $\Gamma X\perp$ geometry, where the odd main band $\psi(\mathbf{k})$ and the odd SL band $\psi(\mathbf{k} + \mathbf{Q}) + \psi(\mathbf{k} - \mathbf{Q})$ should contribute. The results are plotted in the inset to Fig. 2(b).

The odd state disperses more rapidly than the even one with the peak positions corresponding quite well with the expected odd main and even SL bands. No evidence for the odd SL band is found; the reason for this is not clearly understood, but it could be a final state effect.

In the third panel [Fig. 1(3)] the data correspond to a polarization $\Gamma X\|$ with $h\nu = 19$ eV. We see a SL peak, at -300 meV at the Γ point, which disperses through E_F a third of the way from Γ to $\overline{M}$ [see Fig. 2(a)]. The intense spectral peak is the main band dispersing towards E_F but staying just below it at a binding energy of -30 meV, corresponding to an extended saddle point singularity.

We have carefully ascertained the absence of a FS crossing for the main band along $\Gamma\overline{M}$ by studying the momentum derivative of the energy-integrated intensity [10], $|\nabla_{\mathbf{k}} n(\mathbf{k})|$, and found no sharp feature in $n(\mathbf{k})$. This implies that the bilayer splitting of the CuO_2 bands does not lead to two Fermi surfaces, one of which is closed about Γ. We will return to this important point below.

The main band, which is flat along $\Gamma\overline{M}$, shows a clear FS crossing along $\overline{M}X$ in the fourth panel [Fig. 1(4)]. From the FS curves in Fig. 2(a) one might have expected to see a second crossing along $\overline{M}X$ corresponding to a SL band. However, none is seen because the very intense main band masks it. Also note the rather large nondispersive "background" emission near X, which seems to persist long after the main peak has crossed E_F. Its origin is not clear; a possible source might be higher order umklapps from the incommensurate SL.

Finally, we turn to panel five [Fig. 1(5)]. For $\Gamma\overline{M}\perp$ we suppress the main band contribution (which dominated in panel three), since a $d_{x^2-y^2}$ one-particle state is even about $\Gamma\overline{M}$ [17]. We see a weak signal crossing E_F, which is precisely what we would expect for the SL band; see the correspondence of this data point with the curves in Fig. 2. This explains the FS crossing observed previously in only this polarization [18] and interpreted as evidence for a FS sheet closed around Γ. In the upper part of this panel one turns the corner at $\overline{M}$ and finds a main band E_F crossing along $\overline{M}Y$ at a location similar to that along $\overline{M}X$.

As stressed in the introduction we expect *two* CuO_2 bands in a bilayer material; however, in the normal state data we see only one. We now show that even in the SC state, where one has a better ability to resolve the bilayer splitting, we see no evidence for it. We begin by summarizing the band theory predictions [19]. Two resolvable Fermi surfaces are *not* necessarily expected; this depends sensitively on the exact doping levels and on the presence of Bi-O pockets, which are neither treated accurately in the theory nor observed in the ARPES data. However, there is a clear prediction [19] that at $\overline{M}$, where both bands are below E_F, the bilayer splitting is the largest, of order 0.25 eV. Such a splitting should be observable (below T_c) even if there was a moderately large many-body renormalization.

We show in Fig. 3 data at $\overline{M}$ in the SC state at $T = 13$ K. The collapse of the linewidth with decreasing temperature and the appearance of a sharp resolution limited peak at –30 meV was discussed in Ref. [10]. Here we focus on the second bump at -100 meV and the dip which separates it from the first peak. We must now choose between two hypotheses: (A) The dip feature is a many-body effect in a single spectral function $A(\mathbf{k}, \omega)$, the ARPES intensity being proportional to $|\langle\psi_f|\mathbf{A}\cdot\mathbf{p}|\psi_i\rangle|^2 f(\omega)A(\mathbf{k}, \omega)$; (B) the dip feature arises from two bilayer split bands which are resolved below T_c once one of the spectral features becomes sharp. The ARPES intensity in this case would be the sum of two pieces each of which have the same form as in case (A).

By changing the incident photon direction, and thus $\mathbf{A}$, with respect to the z axis, we directly affect the dipole matrix element. Since there is only one matrix element involved in case (A), upon proper rescaling both spectral features in the EDC's should match as $\mathbf{A}$ is varied. However, for case (B) there are two independent matrix elements which should vary differently with $\mathbf{A}$, and thus if the EDC's are scaled so that one of the spectral peaks matches, the other should differ significantly.

We see from Fig. 3 that for Bi2212 hypothesis (A) is valid and the dip and two peaks are all part of a single spectral function. A very natural many-body explanation of the dip has been proposed [20], which leads to a suppression of the linewidth for $\omega < 3\Delta$. We have found that such a linewidth is able to account for the observed features in the spectrum and defer detailed fits to a later publication. We note that a many-body interpretation of the dip is also consistent with the observation of Zasadzinski *et al.* [21] that the dip in point-contact tunneling spectra scales with

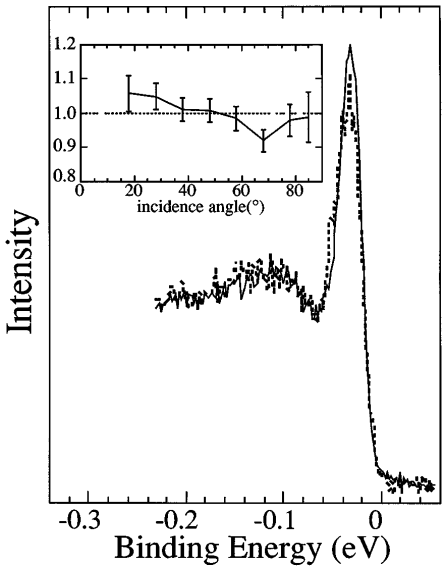

FIG. 3. Low temperature ($T = 13$ K) EDC's of Bi2212 at $\overline{M}$ for various incident photon angles. The solid (dashed) line is 18° (85°) from the normal. The inset shows the height of the sharp peak for data normalized to the broad peak at different incident angles.

the gap in a number of cuprates (some of which have only one layer per unit cell).

Finally, we contrast YBCO [2,7,8] with Bi2212. Early dispersion data gave some evidence for bilayer split bands in YBCO. The leading peak for YBCO is sharp, but the second spectral feature never sharpens even as it approaches E_F. While the data show no sign of a gap, the overall shape of the spectrum looks similar to the Bi2212 SC state data. For specific photon energies ($h\nu = 28$ eV) the first peak, but not the second one, can be resonantly enhanced, which suggests independent matrix elements associated with the two spectral features in YBCO. Further work on YBCO analogous to that of Fig. 3 would be of interest to further address this point.

In conclusion, we have shown that the electronic excitations of Bi2212 are consistent with the absence of bilayer splitting. This observation has important implications for any microscopic theory of high temperature cuprate superconductors, and puts an even stronger constraint than the observation of incoherent *c*-axis transport which only probes the (weaker) coupling of one bilayer to another.

We acknowledge stimulating conversations with P. W. Anderson and R. Liu. This work was supported by the U.S. Dept. of Energy, Basic Energy Sciences, under Contract W-31-109-ENG-38. The Synchrotron Radiation Center is supported by NSF Grant No. DMR-9212658.

[1] C. G. Olson *et al.,* Science **245**, 731 (1989); Phys. Rev. B **42**, 381 (1990).
[2] J. C. Campuzano *et al.,* Phys. Rev. Lett. **64**, 2308 (1990).
[3] Z. X. Shen and D. S. Dessau, Phys. Rep. **253**, 1 (1995).
[4] P. Aebi *et al.,* Phys. Rev. Lett. **72**, 2757 (1994); J. Osterwalder *et al.,* Appl. Phys. A **60**, 247 (1995).
[5] P. W. Anderson, Science **256**, 1526 (1992).
[6] D. S. Dessau *et al.,* Phys. Rev. Lett. **66**, 2160 (1991).
[7] R. Liu *et al.,* Phys. Rev. B **45**, 5614 (1992); **46**, 11 056 (1992).
[8] K. Gofron *et al.,* J. Phys. Chem. Solids **54**, 1193 (1993); Phys. Rev. Lett. **73**, 3302 (1994).
[9] H. Ding *et al.,* Phys. Rev. Lett. **74**, 2784 (1995).
[10] M. Randeria *et al.,* Phys. Rev. Lett. **74**, 4951 (1995).
[11] M. R. Norman *et al.,* Phys. Rev. B **52**, 615 (1995).
[12] R. L. Withers *et al.,* J. Phys. C **21**, 6067 (1988).
[13] A. Kampf and J. R. Schrieffer, Phys. Rev. B **42**, 7967 (1990).
[14] Bi2212 has a face-centered orthorhombic cell with two inequivalent Cu sites per plane, which by itself could generate a (π, π) foldback.
[15] J. Ma *et al.,* Phys. Rev. B **51**, 9271 (1995).
[16] H. Ding *et al.,* Phys. Rev. Lett. **75**, 1425E (1995) (erratum to Ref. [9]).
[17] Strictly speaking $\Gamma\overline{M}$ is not a mirror plane in the presence of a SL distortion. However, to the extent that the Bi-O SL only diffracts the outgoing photoelectron at the surface, within a "three-step" model, $\Gamma\overline{M}$ *is* a mirror plane for a final state on the CuO_2 plane.
[18] D. S. Dessau *et al.,* Phys. Rev. Lett. **71**, 2781 (1993).
[19] S. Massida, J. Yu, and A. J. Freeman, Physica (Amsterdam) **152C**, 251 (1988); O. K. Andersen *et al.,* Phys. Rev. B **49**, 4145 (1994).
[20] C. M. Varma and P. B. Littlewood, Phys. Rev. B **46**, 405 (1992); L. Coffey and D. Coffey, Phys. Rev. B **48**, 4184 (1993).
[21] J. Zasadzinski *et al.* (unpublished); see Fig. 1 of D. Coffey, J. Phys. Chem. Solids **54**, 1369 (1993).